Scaling of the number of modes in mode division multiplexing systems

Filipe M. Ferreira, ***Senior Member, IEEE,*** **Fabio A. Barbosa,** ***Member, IEEE, Rekha Yadav, Zun Htay***

Optical Networks, Dept. Electronic & Electrical Eng., University College London, UK
e-mail: f.ferreira@ucl.ac.uk

ABSTRACT
We review our recent advances on the design of multimode fibres with hundreds of spatial pathways for reduced differential mode delay in the C-band and on the development of adaptable spatial multiplexing techniques to enable scalability of all data pathways.
Keywords: multimode fibres, space division multiplexing, differential mode delay.

1. INTRODUCTION

Space-division multiplexing (SDM) has emerged as a solution to overcome the capacity limit of single-mode fibres (SMFs). Among the possible SDM approaches, multimode fibres (MMFs) offer the highest spatial information density followed by coupled-core multicore fibres (MCFs) and with bundles of SMFs and uncoupled-core MCFs on the other end. However, the multitude of spatial modes introduces new linear impairments, namely group delay (GD) spread [1] given the interplay between differential mode delay (DMD) and linear mode coupling (LMC), and mode dependent loss (MDL) [2]. The GD spreading can be overcome using MIMO equalisation but with complexity scaling linearly with the total time spread while MDL introduces a fundamental loss of throughput. Therefore, multimode SDM fibres are designed with a graded-index core [3] to reduce the DMD and with a cladding trench to increase the confinement of the higher-order mode groups and in this way reduce MDL [1]. However, as it is shown further on, higher DMD and MDL must be allowed to be able to scale the number of guided modes. Ultimately, MDL will introduce a bound to the throughput achievable and DMD will set equalisation complexity for mode division multiplexing to approach such throughput bounds.

In the following, we review our recent progress on the scaling of the number of modes by increasing the fibre core diameter and core-cladding contrast while optimising all the parameters in a trench-assisted graded-core refractive-index profile [2]. For these optimised fibres, the throughput scaling is investigated taking into account all major loss sources, Rayleigh scattering loss, macro-bend and coating loss. Finally, we review the equalisation complexity scaling required to approach such throughput bound [3].

2. FIBRE DESIGN AND OPTIMISED DMD

Fig. 1 shows the fibre profile considered. There are six design parameters available: the core graded exponent, α, the core and trench relative refractive index, Δn_{co} and Δn_{tr}, respectively, the core radius w_1, the trench to the core distance, w_2,, and the trench width, w_3. To optimise over this 6-D space, one can exploit the parameters interdependence and on how these impact key figures of merit, including the number of modes, DMD and/or MBL. The number of modes N scales with w_1 and Δn_{co}, and is approximately given by $2N \approx V^2/2 \cdot [\alpha/(\alpha+2)]$ – where V is the normalised frequency $V = 2\pi w_1/\lambda \cdot [n_{co}^2 - n_{cl}^2]$. However, increasing w_1 and/or Δn_{co} leads to a degradation of key transmission characteristics, such as MDL and DMD. The larger w_1 becomes in a 125 μm cladding diameter (wider claddings are mechanically unreliable), the larger the macro-bend loss [4] as the confinement of the higher-order mode groups reduces. And the larger Δn_{co}, the larger the Rayleigh scattering loss – modes with greater core confinement and so greater overlap with Ge-dopants experience greater scattering. Moreover, the larger Δn_{co}, the larger DMD – the spread of modes effective index scales with Δn_{co} [5]. For a given Δn_{co}, DMD is 1st determined by the core grading exponent α [1, 5, 6], and 2nd by the trench dimensioning. The

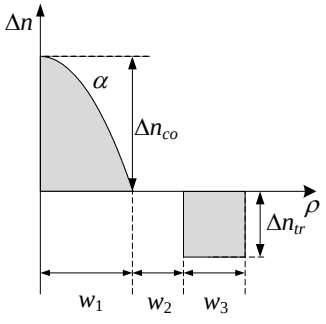

Figure. 1. GI profile with cladding trench. ρ is the polar radial coordinate.

$$\begin{aligned} \Delta n_{co}\cdot 100 &\in \{0.5 : 0.5 : 5\} \\ \Delta n_{tr}\cdot 100 &\in \{-1.3 : 1/40 : 0\} \\ \alpha &\in \{1.92 : 0.1/40 : 2.05\} \\ w_1 &\in \{10 : 5 : 50\}\ (\mu m) \\ w_2 &\in \{2\}\ (\mu m) \\ w_3 &\in \{6\}\ (\mu m) \end{aligned} \quad (1)$$

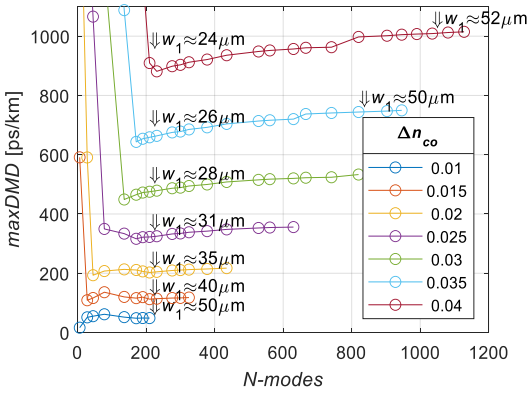

Figure. 2. *maxDMD* [ps/km] as a function of *N*-modes for different Δn_{co}. The last point in each line corresponds to w_1 = 50μm. Note that: w_1 given *N* workable via $N \approx V^2/4 \cdot [\alpha/(\alpha+2)]$.

latter plays a particular role in the mode delay slope with wavelength for the higher-order modes, as show in [6].

The trench dimensions (w_2, w_3, Δn_{tr}) are particularly interdependent. For example, relatively speaking, a narrow and deep trench can have the same impact on DMD as a wider and shallower trench. Having previously shown that (α, Δn_{tr}) form a convex space (given w_1, w_2, w_3, Δn_{co}) [6], a finer search step is applied to Δn_{tr} while a coarser step is applied to (w_2, w_3). Moreover, it was found that w_2 = 2 μm and w_3 = 6 μm allow for (quasi-)optimum DMD for the w_1 and Δn_{co} of most interest. In the following, (w_2, w_3) are not optimised and simply hold at w_2 = 2 μm and w_3 = 6 μm. All parameter search constrains in (1).

To optimise for miminum DMD, the optimization function chosen is given by the maximum DMD (*maxDMD*) among the guided modes (here, linearly polarised modes, $LP_{\mu\nu}$) over the C-band: $maxDMD(p) = \max_{\lambda}(\max_{\mu\nu}|DMD(\lambda,\mu\nu)|)$, where $p = [\alpha, \Delta n_{co}, \Delta n_{tr}, w_1, w_2, w_3]$, and $DMD(\lambda,\mu\nu)$ is the group delay difference between mode $LP_{\mu\nu}$ and the reference mode chosen (e.g., LP_{01}). The objective function is subject to the constrains given in (1) over which exhaustive search is performed. The constraints in (1) aim to reflect the knowledge that near-parabolic are optimal (i.e., α), the limitations in fabrication, and the asymmetric capabilities in Ge- and in F-doping (i.e., for greater Δn_{co} and $|\Delta n_{tr}|$) [7]. The solutions to the waveguide defined by *p* are found using the vector finite difference solver developed in [8] – a grid step of 0.2μm and grid size of $4 \cdot (w_1+w_2+w_3)$ is used (twice finer grids led to negligible change). The dispersion properties of pure, Ge-doped or F-doped silica have been modelled using the Sellmeier coefficients provided in [9].

Fig. 2 shows *maxDMD* as a function of *N*-modes for several Δn_{co} values – considering for optimum (α, Δn_{tr}) pair in each w_1 case. For each Δn_{co} there is a *maxDMD* plateau along which a *N*-modes increase without a *maxDMD* degradation. But note that for small *N*-modes (w_1) the fixed trench position and width are no longer near optimum (instead closer, narrower and deeper trenches would be necessary). In any case, we seek to maximise *N*-modes, thus the results for smaller w_1 are disregarded. Fig. 2 shows that higher Δn_{co} allows an increasingly higher *N*-modes (bounded by the 125μm cladding) but at the cost of a higher *maxDMD* – as expected. It scales from *N* = 210 (20 mode groups) with *maxDMD* ≈ 50 ps/km at $\Delta n_{co} \cdot 10^2 = 1$, through *N* = 630 (35 mode groups) with 355 ps/km at $\Delta n_{co} \cdot 10^2 = 2.5$, and all the way up to *N* = 1128 (47 mode groups) with 1014 ps/km at $\Delta n_{co} \cdot 10^2 = 3$. The practical impact of DMD on SDM throughput is well understood in terms of conventional MIMO equalisation complexity – fibres with *maxDMD* >150ps/km in Fig. 2 are potentially suited for mode group multiplexing exploiting the reduced intra-mode group DMD.

3. CHANNEL THROUGHPUT

The channel transfer function $H[f]$ (for each optimised fibre) is a $2N \times 2N$ matrix calculated for a single span of 100 km using the multi-section model in [10]. A 128-point frequency vector is considered to account for the frequency dependent response along the C-band (1530-1565 nm, 5 THz). The calculation of *H* considers all main linear impairments, this is Rayleigh scattering, MBL, DMD and LMC – along 100 fibre sections. The MBL corresponding to one 30 mm radius turn is applied in every fibre section. And finally, random LMC is introduced every fibre section given a core-cladding boundary displacement of 0.06μm and a uniformly distributed azimuthal displacement (a stronger radial offset does not change the conclusions). Such core-cladding imperfections are typical of manufactured MMF fibres [7]. Fig. 3 shows a typical $|H|^2$ in dB scale, where $|\cdot|^2$ is applied element-wise. As expected, the LMC strength is significantly higher between neighbouring mode groups – given closer mode effective index and stronger mode overlap.

Using MIMO theory [11], information throughput is computed by decomposing $H[f]$ into a set of parallel, independent scalar Gaussian sub-channels through a singular value decomposition (SVD). This is,

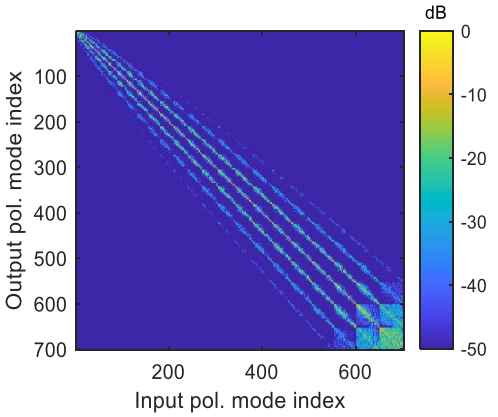

Figure. 3. Example H (at $f = 0$) for a fibre with 25 mode groups.

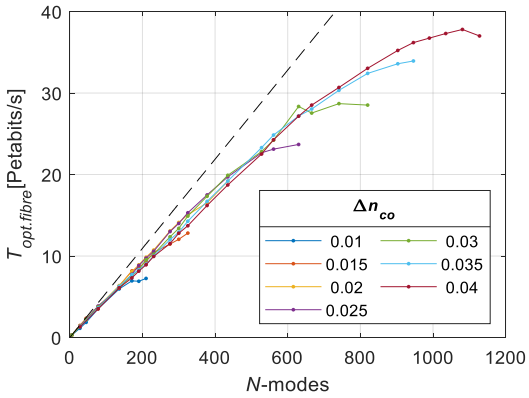

Figure. 4. Throughput as a function of N-modes for several Δn_{co} – same fibres of Fig. 2.

$H[f] = U[f]S[f]V[f]^{H}$, where U and V are unitary matrices and S is a diagonal matrix whose diagonal elements $\lambda_1^{[f]}$, …, $\lambda_{2N}^{[f]}$ are non-negative real numbers and whose off-diagonal elements are zero. Each non-zero eigenmode $\lambda_i^{[f]}$ can support a data tributary, $i = 1, \ldots, n_{NZ}$. In this way, a throughput bound T, assuming full channel state information, is given by: $T = \sum_{f = -64:63} (5\text{ THz} / 128) \sum_{i = 1 : n_{NZ}} \log(1 + P_i^{[f]} \lambda_i^{[f]2} / N_0)$ bits/s, where $P_1^{[f]}$, …, $P_{n_{NZ}}^{[f]}$ are the waterfilling power allocations $P_i^{[f]} = (\mu + N_0 / (\lambda_i^{[f]})^2)^+$ for frequency channel f, with μ chosen to satisfy the total power constraint $\sum P_i^{[f]} = P$, and $(\cdot)^+$ is zero if its argument is negative. We choose N_0 such that the lowest loss mode has a signal-to-noise (SNR) of 17 dB which is compatible with 100 km transmission in a power-limited scenario.

Fig. 4 shows throughput as a function of the number of modes for several Δn_{co} – same optimum fibres of Fig. 2. A maximum throughput around 35 Petabit/s can be observed (given the profile constraints in (1) and SNR conditions considered). Moreover, the spatial multiplexing gain significantly deviates from a 1-to-1 linear gain given the increase in MDL – driven mostly by Rayleigh scattering loss. Therefore, it might be more efficient (e.g. energy wise) to design for a lower Δn_{co} and so lower number of modes. To reach the throughputs discussed, receiver memory (and so complexity) must accommodate the delay spread in the channel.

4. EQUALISATION COMPLEXITY

Conventional MDM transmission requires all guided modes to be detected for successful MIMO equalisation, otherwise outage probability becomes unpractical. Having the number of transceiver front-ends following that of fibres modes prevents the installation of many mode MMFs, since at begin-of-life it would not be economically viable to deploy transceivers with as many front-ends – a pay as you grow model similar to WDM systems would be desirable. We have recently proposed a transceiver architecture based on principal modes (PMs) which allows for the number of spatial tributaries and that of transceivers front-ends to scale equally [3]. Using PMs requires the exchange of channel state information (CSI) between the transmitter and receiver, making this architecture vulnerable to environment induced channel drift. In [3], we numerically investigate the use of PMs for a much larger number of spatial and polarisation modes, $M = 342$, under mode dependent loss and modal dynamics, and a varying rate of perturbations, while accounting for delay in the CSI feedback.

In theory, PMs should allow for crosstalk free transmission within a given coherence bandwidth. However, mode dependent loss (arising from Rayleigh scattering, macro-bend and coating loss) and environmental induced channel drift reduce the orthogonality of the PMs. Therefore, channel equalisation will be required even when using PMs. To translate XT into the required multiple-input-single-output (MISO) array size per tributary, we count the *interfering terms* that need compensation to achieve a given target signal-to-noise ratio (SNR) – the weaker *interfering terms* are neglected. This is done by neglecting the smallest group of *interfering terms* that amounts to a XT below a certain threshold. In [3], the threshold was set to $XT \leq$ -20 dB such that after applying the required MISO, an SNR of 20dB is achievable should the channel additive noise allow. Fig. 5 shows the MISO array size for each PM pair in a group of N_T-PM pairs, for a channel with a characteristic timescale of change $\tau_{env} = 48$s – this is, after τ_{env} the fibre transfer matrix is fully decorrelated (simulation considers a 10km fibre with 10m sections, applying drift to all sections [12]). In the figure, it can be seen that for groups with 22, 42, 82, 122 and 182 PM pairs, single-input single-output (SISO) equalisation is sufficient for recovering the transmitted signals under the assumptions made in terms of XT and SNR. And, for groups with more than 182 PM pairs, MISO equalisation is necessary, although the maximum array size required for a given group, is at least an order of magnitude smaller than N_T. Note that, a linear scaling of the MISO array size would be for every PM pair in a group of N_T to require a MISO array size of N_T, i.e. $N_T \times N_T$ MIMO.

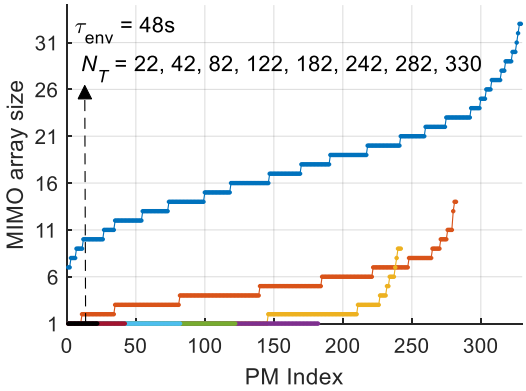

Fig. 5. MISO array size required per PM pair to detect all data tributaries in a N_T-group, for an increasing number of tributaries N_T. Results are sorted in ascending order for visualization purposes.

5. CONCLUSIONS

We review advances on the design of graded-index trench-assisted multimode fibres supporting over 1000 LP modes (and twice as many polarizations modes) for minimum differential mode delay in the C-band. It was shown that over 400 LP modes can be supported within a maximum differential mode delay of 250 ps/km, typical of OM fibres at 850 nm. And that, for a given core-cladding contrast, the number of modes can be scaled by increasing the core radius without significant degradation of the differential mode delay.

We have quantified how throughput scales with the number of modes taking into account the impact of Rayleigh scattering, macro-bend and coating loss, as well as linear mode coupling. It was shows that as much as 35 Petabits/s over 100 km can be achieved assuming *SNR* ~17dB. However, for refractive-index contrasts beyond 0.04, throughput scaling was shown to enter a strong diminishing returns regime.

The MISO array size requirements to approach such throughputs were also reviewed making clear the advantages of a principal modes-based approach. This architecture opens pathways to a transceiver architecture with the number of front ends following that of tributaries even when using a subset of the total number of modes available in the fibre. Importantly, with the total MISO complexity accounting for only a fraction of the equalisation complexity for full *N*x*N*-MIMO.

ACKNOWLEDGEMENTS

This work was supported by the UKRI Future Leaders Fellowship MR/T041218/1. For the underlying data, see: doi.org/10.5522/04/19739038, and doi.org/10.5522/04/21360492.

REFERENCES

[1] F. Ferreira, D. Fonseca, and H. Silva, "Design of few-mode fibers with arbitrary and flattened differential mode delay," *IEEE Photonics Technology Letters*, vol. 25, no. 5, p. 438, 2013, doi: 10.1109/LPT.2013.2241047.

[2] F. M. Ferreira and F. A. Barbosa, "Towards 1000-mode Optical Fibres," 2022.

[3] F. A. Barbosa and F. M. Ferreira, "On the advantages of principal modes for multimode SDM transmission systems," in *Optical Fiber Communication Conference (OFC) 2023*, p. Th2A.31.

[4] J.-i. Sakai and T. Kimura, "Bending loss of propagation modes in arbitrary-index profile optical fibers," *Appl. Opt.*, vol. 17, no. 10, p. 1499, 1978, doi: 10.1364/AO.17.001499.

[5] D. Gloge and E. A. J. Marcatili, "Multimode theory of graded-core fibers," *The Bell System Technical Journal*, vol. 52, no. 9, p. 1563, 1973, doi: 10.1002/j.1538-7305.1973.tb02033.x.

[6] F. Ferreira, D. Fonseca, and H. J. A. Silva, "Design of few-mode fibers with M-modes and low differential mode delay," *J. Light. Technol.*, vol. 32, no. 3, p. 353-, 2014, doi: 10.1109/JLT.2013.2293066.

[7] A. Bourdine, D. Praporshchikov, and K. Yablochkin, *Investigation of defects of refractive index profile of silica graded-index multimode fibers* (Optical Technologies for Telecommunications 2010). SPIE, 2011.

[8] A. B. Fallahkhair, K. S. Li, and T. E. Murphy, "Vector Finite Difference Modesolver for Anisotropic Dielectric Waveguides," *J. Light. Technol.*, vol. 26, no. 11, p. 1423, 2008, doi: 10.1109/JLT.2008.923643.

[9] W. Hermann and D. U. Wiechert, "Refractive index of doped and undoped PCVD bulk silica," *Materials Research Bulletin*, vol. 24, pp. 1083-1097, 1989.

[10] F. M. Ferreira, C. S. Costa, S. Sygletos, and A. D. Ellis, "Semi-Analytical Modelling of Linear Mode Coupling in Few-Mode Fibers," *J. Light. Technol.*, vol. 35, no. 18, p. 4011, 2017, doi: 10.1109/jlt.2017.2727441.

[11] D. Tse and P. Viswanath, *Fundamentals of Wireless Communication*. Cambridge: Cambridge University Press, 2005.

[12] K. Choutagunta, I. Roberts, and J. M. Kahn, "Efficient Quantification and Simulation of Modal Dynamics in Multimode Fiber Links," *J. Light. Technol.*, vol. 37, no. 8, pp. 1813, 2019, doi: 10.1109/JLT.2018.2889675.